

# Synoptic study of warm rings in the North Brazil Current retroflection region using satellite altimetry

Gustavo J. Goni<sup>a\*</sup> and William E. Johns<sup>b</sup>

<sup>a</sup>National Oceanic and Atmospheric Administration,  
Atlantic Oceanographic and Atmospheric Laboratory,  
4301 Rickenbacker Causeway, Miami, Florida 33149, USA.

<sup>b</sup>University of Miami, Rosenstiel School of Marine and Atmospheric Science,  
Miami, Florida 33149, U.S.A.

Ten years of altimeter data are used in conjunction with temperature and salinity data within a two-layer reduced gravity approximation to investigate the shedding and translation of North Brazil Current rings. Space-time diagrams of sea height anomalies and residues along the altimeter groundtracks show large seasonal and interannual variability. Results presented here confirm previous estimates that indicate a shedding rate of 3 to 7 rings per year with no marked seasonal variability but with very strong year-to-year variability. Additionally, eddies not shed by the retroflection travel through the region as well. Most of the rings pass very near of Barbados, affecting the environment in the region, of which seven rings during the study period are seen to enter into the Caribbean Sea. A link is found in this study between long-term surface temperature changes in the tropical Atlantic and the number of rings shed at the NBC retroflection, where periods of time with warmer surface temperatures are associated to a higher number of rings shed.

## 1. INTRODUCTION

The investigation of the upper ocean heat balance in the equatorial Atlantic is concentrated in the cross-equatorial exchange of near surface waters that make up the upper limb of the Meridional Overturning Circulation. Waters from the South Atlantic subtropical gyre cross through the equatorial circulation system to finally enter into the North Atlantic subtropical gyre. The wind-driven patterns in the tropical Atlantic are complex and contribute to the three dimensional circulation, as in the case of the equatorial upwelling and off-

---

\*Corresponding author; Tel: 305-361-4339, Email: Gustavo.goni@noaa.gov

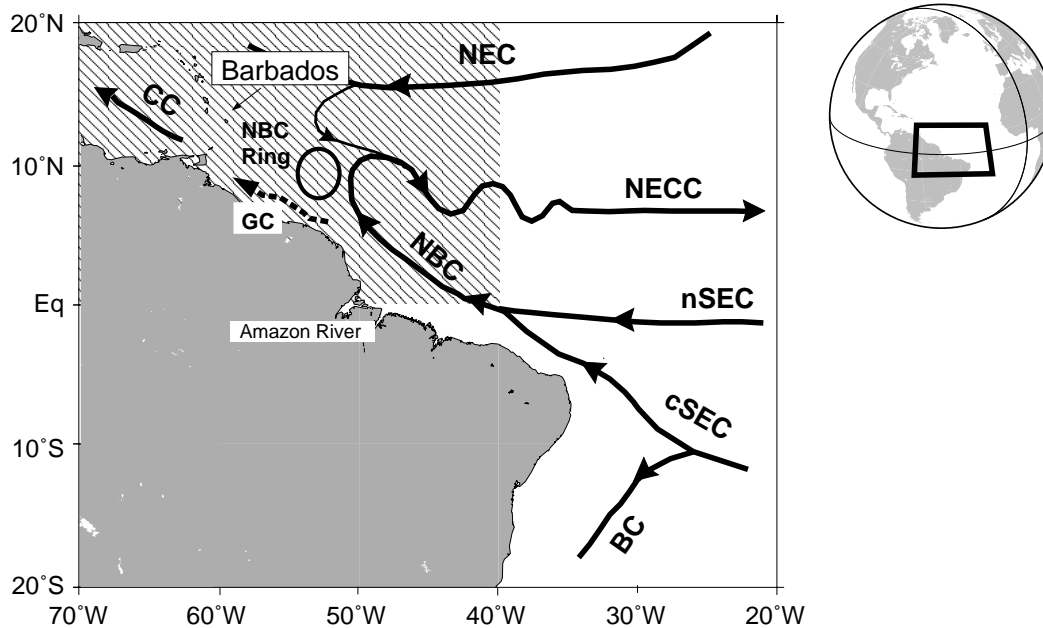


Figure 1. The region of study indicating the main surface current in the tropical Atlantic, the central South Equatorial Current (cSEC), the Brazil Current (BC), the north South Equatorial Current (nSEC), the North Brazil Current (NBC), the Guyana Current (GC), the North Equatorial Counter Current (NECC), the North Equatorial Current (NEC) and the Caribbean Current (CC). The shaded area indicates the region where the NBC rings are investigated in this study.

equatorial downwelling. Southern hemisphere water makes its way into the North Atlantic through two primary pathways: rings shed by the low latitude North Brazil Current (NBC) as it retroflects into the interior, and seasonal rectification of the upper layer currents that allow warm surface waters to be stored in the North Equatorial Counter Current (NECC)/North Equatorial Current (NEC) ridge system and released northward via Ekman transports (Mayer and Weisberg, 1993).

The North Brazil Current is a northward flowing western boundary current that carries warm waters across the Equator off the easternmost tip of Brazil and along the coast of South America (Figure 1). The origin of this current is linked to the bifurcation of the SEC, particularly its central branch (cSEC), which contributes to the formation of the north flowing NBC and the south flowing Brazil Current (Schott *et al*, 1998). The NBC retroflects between 5 and 10°N (Johns *et al*, 1990) shedding warm anticyclonic rings, among the largest warm rings in the oceans. Early studies showed that this retroflexion occurs mostly during the boreal summer and fall months, and that its waters join the NEC (Molinari and Johns, 1994). The warm rings shed by the NBC then become one of the mechanisms that contributes to the transport of South Atlantic upper waters into the northern hemisphere. These rings travel in a NW direction partly carried by the background current (Guyana Current) and partly by their

own translation speed. These rings either enter the Caribbean Sea or the North Atlantic subtropical gyre as part of the Atlantic meridional overturning cell (Johns *et al.*, 1998). The countercurrents, rings and meanders found in the region of the NBC retroflection contribute to the regional variability, which is investigated here using satellite altimetry.

The vertical thermal structure of this region has been used to identify mesoscale features and the mass transport using hydrographic data. Reverdin *et al.* (1991) used the 11°C and 20°C isotherm to represent thermocline displacements to investigate the variability of the deep thermocline. Molinari and Johns (1994) investigated the variability and annual and semiannual cycles of the 20°C and 10°C isotherms in the region from historical XBT data. They concluded that the annual and semiannual harmonics account for more than 60% of the total variance in the region. Didden and Schott (1993, DS93 hereafter) used Geosat altimeter data during 1986-1989 to carry out a study of these warm rings based on the sea height anomaly data and concluded that 2 to 3 rings were detached from the NBC retroflection from November through January. Fratantoni *et al.* (1995) also carried out a detailed investigation using near subsurface velocity and temperature measurements, model results and the same Geosat-derived sea height anomaly data used by DS93. Their model and altimetry results showed ring formation limited approximately to December to March, while the velocity fields derived from Acoustic Doppler current profilers show rings translating in the region during the whole year. Goni and Johns (2001, GJ01) later used a six year long (1993-1998) TOPEX/Poseidon altimeter data set to create an expanded census of NBC rings, which represented the first long time series of these features. Results from this work indicated that 2 to 6 rings were formed each year without any marked seasonality and that these rings may account for up to 1/3 of the meridional mass transport across the Equator in the Atlantic Ocean. Most recently, Fratantoni and Glickson (2002) identified 18 NBC rings during a three-year period (September 1997 through September 2000) using ocean color imagery, confirming the larger number of rings shed and a the lack of a marked seasonability in their formation. Observations and models indicate that there are at least three types of rings shed by the NBC retroflection: surface, deep and subsurface (Wilson *et al.*, 2002). Other chapters in this book (Garraffo *et al.* and Johns *et al.*) include references and results on these different types of rings. It is important to mention at this point that the existence of subsurface NBC rings was being reproduced in numerical models before they were actually first observed. These subsurface rings have a small or vanishing sea surface height signal and are a relatively new discovery. The reader is referred to these chapters to complement and enhance the information provided here, particularly to compare with model results (Garraffo *et al.*), inverted echo sounder observations (Garzoli *et al.*) and on the effect of the NBC rings on Barbados (Cowen *et al.*).

Two altimeter data sets are used here, one corresponding to the TOPEX/Poseidon (T/P) altimeter and another to a blended data set of three altimeters, TOPEX/Poseidon, the ESA Remote Sensing-2 Satellite 2 (ERS-2) and

the Geosat Follow-On (GFO). Results presented in this chapter correspond to the period November 1992 through December 2001. The rings in this work are identified and tracked using the same procedure as described in Goni and Johns (2001). A long period signal in the sea surface temperature data in the tropical Atlantic is also used to explore a possible link between this signal and the formation of NBC rings.

## 2. REGION OF STUDY

The region of study extends from 40°W to 70°W, and from 0 to 20°N (Figure 1), which is characterized by the presence of a warm and salty current, the North Brazil Current, which retroflects at approximately 45°W 5°N. While this current retroflects it sheds warm anticyclonic rings that propagate in a NW direction off the coast of South America until reaching the Windward Islands, where they disintegrate, cross into the Caribbean or continue with a northward propagation (DS93; GJ01). Waters from the Amazon River are embedded in the retroflexion region. The NBC rings are known to carry fresher waters from the Amazon River causing marked influence on the environmental conditions surrounding the Windward Islands, particularly Barbados (Kelly, 2001 and Cowen *et al*, this volume).

## 3. DATA

The three main data sets used in this study are:

1. Altimeter-derived sea height anomaly. Alongtrack TOPEX/Poseidon data from November 1992 onward is used throughout this work, while blended alongtrack data from TOPEX/Poseidon, ERS2 and GFO since 1998 is used, and only to create maps with improved spatial resolution to better identify NBC rings.
2. 1x1 degree temperature and salinity data from the Levitus climatology (Conkright *et al*, 1998) is used to obtain the mean depth of the 20°C isotherm and reduced gravity fields.

### 3.1. Altimeter data

The altimeter-derived sea height anomaly,  $\eta'$ , is the value of the deviation of the actual sea height,  $\eta$ , referred to the mean sea height,  $\bar{\eta}$ , which is computed over a period of time of several years:

$$\eta'(x, y, t) = \eta(x, y, t) - \bar{\eta}(x, y). \quad (1)$$

The altimeter measures the sea height anomaly along the altimeter groundtracks (Figure 2), providing data that is distributed irregularly in space

and time. Adjacent T/P, GFO and ERS-2 groundtracks are separated approximately 3, 2 and 1 degrees longitudinally, respectively, and are repeated

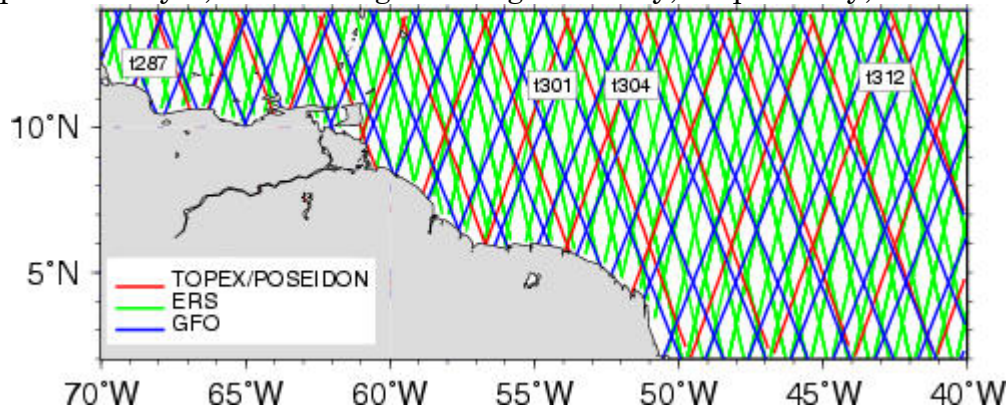


Figure 2. T/P, ERS-2 and GFO altimeter groundtracks in the region of study. Four ascending T/P groundtracks (t287, t301, t304 and t312) are indicated for later reference.

approximately every 10, 17 and 35 days.

The sea height anomaly alone is not always a good indicator of the presence of warm rings, particularly in frontal regions close to where rings are being shed, or in regions where the steric effect on the sea height is comparable to the sea height variations produced by these rings.

In the first case, an alternation of positive and negative sea height anomalies are usually found in frontal regions (Goni *et al*, 1996), making the distinction of a ring and a front very difficult. A warm frontal area can be either identified from its negative or positive sea height anomaly values, depending on where the front is located with respect to its mean position. The sea height of a moving front and its relationship with its sea height anomaly can be explained using synthetic sea height anomalies profiles (Figure 3) shows how a moving warm front causes a variation in the alongtrack sea height anomaly, even when the frontal shape remains unchanged. Assuming that the altimeter groundtrack crosses through the jet of the current, the location of this jet (maximum alongtrack sea height gradient) can usually be set close to the position of the maximum alongtrack sea height anomaly gradient. Similarly, a warm ring can be observed as an alternation of positive and negative anomalies as the ring travel along its path in a region where the sea height variability of the background flow is comparable to the sea height anomaly of the ring. Consequently, the location of the jet of a current or the maximum flow around a ring is not always coincident with the position of the maximum alongtrack sea height anomaly.

The steric effect, with a clear annual cycle, is one important component of the sea height variability in the study region. It is shown later that the amplitude of this annual signal has a very high dependence on location. This is particularly important when a ring is traveling in a region where the mean sea level exhibits

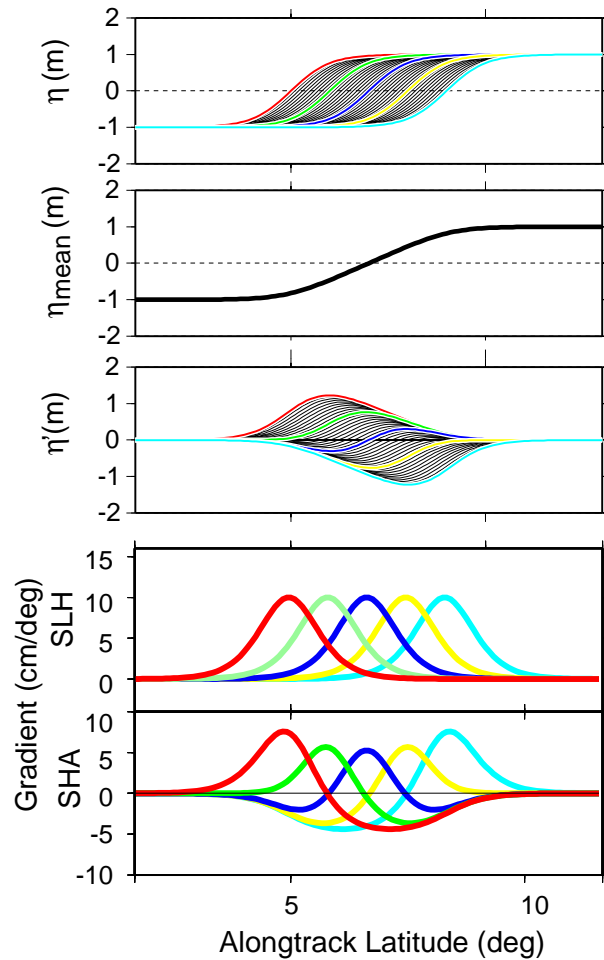


Figure 3. (a) Synthetic sea height profiles simulating a moving front with five individual fronts highlighted. (b) Synthetic mean sea height. (c) Synthetic sea height anomalies. (d) Alongtrack gradients of the synthetic sea height and sea height anomalies.

large spatial variability; the sea height displacement produced by the ring may not be enough to result into a positive sea height anomaly. Therefore, is more appropriate to investigate the rings analyzing their properties referenced to their surrounding waters or having the annual signal removed.

A nine-year altimeter-derived sea height anomaly data set is used in this study to estimate the variability of the sea surface height, with the anomalies referred to the 1993-1998 mean field. The rms of the sea height anomaly (Figure 4) exhibits values ranging from 4 to 11 cm. The regions with higher variability are associated to the North Brazil Current, its rings, to the NECC, and to the variability in the Caribbean Sea. Due to the low latitude setting these rms values are relatively smaller than in other regions where warm anticyclonic rings are also formed. For example, the Brazil-Malvinas Confluence region and

the Agulhas Retroflexion region exhibit maximum rms values of approximately 30 cm (Goni *et al.*, 1996; Goni *et al.*, 1997).

Space-time diagrams represent a useful means to identify and track features in the ocean. They have been successfully used to track warm rings in the region of study using Geosat altimeter data (DS93). The space-time diagram of the sea height anomaly and residues (Figure 5, left and right panels, respectively) for ten selected ascending T/P groundtracks (Figure 2) show very distinctive features. The sea height residual is obtained by subtracting a mean annual and semiannual cycles (Figure 5, middle panel). The steric effects dominated by the annual cycle in the sea height anomaly and the variability of mesoscale features in the sea height residues are the most distinguishable features. The amplitude of the annual cycle ranges from 6 to 12 cm (Figure 6, left panel). The smallest values of annual amplitude, of approximately 3 cm, correspond to the region affected by the passage of the North Brazil Current rings. The annual cycle accounts for approximately 40% of the variability in this area. This value is slightly smaller than the 60% derived from XBT observations (Molinari and Johns, 1994). The semiannual signal accounts for less than 2 cm in most areas in the region of study.

These space-time diagrams and the rms values of the sea height show the very different oceanic conditions east and west of approximately 55°W in terms of both the mean conditions and in the mesoscale variability. The mean annual signal and the sea height residuals reveal very interesting features. First, the annual amplitude (Figure 5, center) is smaller to the east of 55°W and mainly linked to the retroflexion of the NBC, which has a marked annual period (Johns *et al.*, 1990). The residuals show an interannual signal on which the mesoscale signal is superimposed. This signal is of interest in light of a previous work that used Geosat sea height data and reported an increase of the volume of the equatorial upper ocean during 1987-1989, indicative of the effect of the 1986-1987 ENSO (Arnault and Cheney, 1994). This signal of long period and its relationship to NBC ring shedding will be presented later in this chapter.

### 3.2. Climatological data

Climatological temperature and salinity data (Conkright *et al.*, 1998) is used to compute the mean values of the upper layer thickness, which extends from the surface to the depth of the 20°C isotherm, and the reduced gravity for the region of study. The reduced gravity field,  $g'$ , is computed using the mean upper and lower layer densities:

$$g'(x, y) = \varepsilon(x, y)g(y) = \frac{\rho_2(x, y) - \rho_1(x, y)}{\rho_2(x, y)} g(y) \quad (2)$$

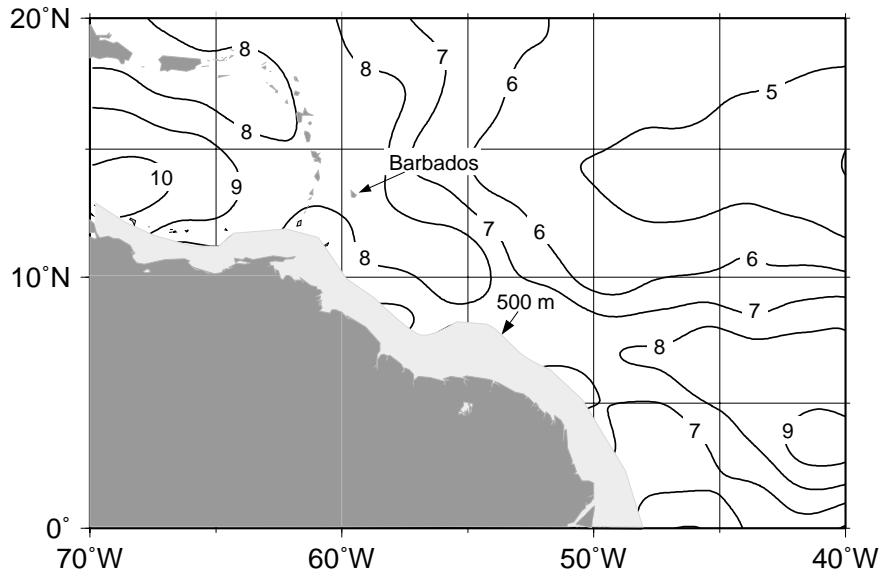


Figure 4. The rms (in cm) of the sea height from TOPEX/Poseidon altimeter data. Rms values for bottom depths shallower than 500 m are masked.

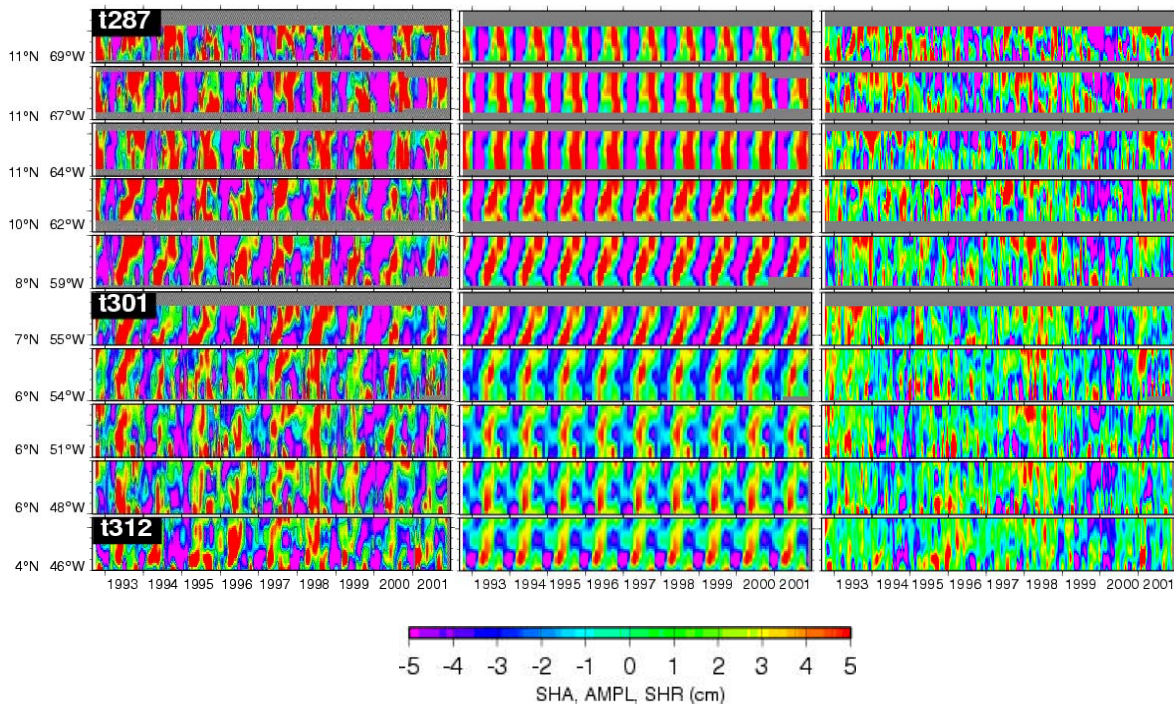


Figure 5. (left) Sea height anomalies for the ascending T/P groundtracks, (center) Annual plus semiannual amplitude of the sea height anomalies, and (right) Sea height residuals for selected ascending T/P groundtracks (see Figure 2). The latitude and longitude of the southern limit of the section of each groundtrack used in these diagrams is indicated on the left, with the sections extending 5 degrees in longitude from west to east.

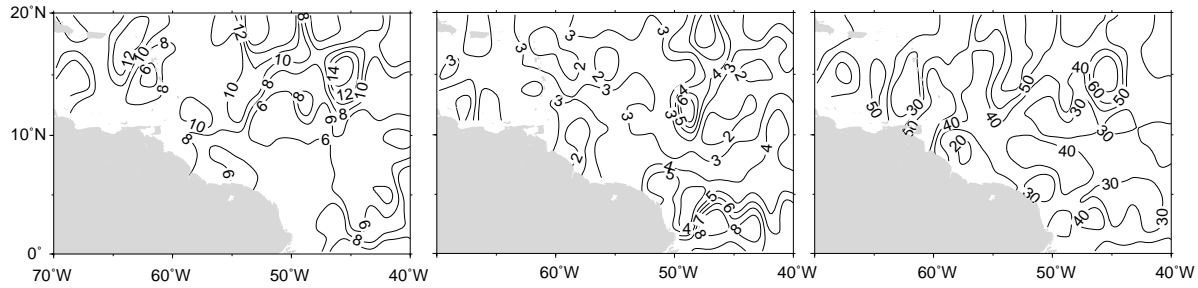


Figure 6. Amplitude of the annual (left) and semiannual (center) cycles and the percentage of variability (right) due to these two cycles obtained using T/P data from 1993 until 2001.

where  $g$  is the acceleration of gravity, and  $\rho_1$  and  $\rho_2$  are the mean densities of the upper and lower layers, respectively. The lower layer is defined as the layer between the depth of the 20°C isotherm and 1500 m or the sea floor. Hence, the reduced gravity provides a measure of the vertical stratification in the region. These climatologically-derived values (Figure 7) are then used in conjunction with the sea height anomalies within a two-layer reduced gravity scheme to obtain the absolute field of the depth of the 20°C isotherm, described next.

#### 4. TWO-LAYER MODEL APPROXIMATION

Some difficulties that arise from using sea height anomaly or residue data to identify and track warm rings have already been discussed. Most of these difficulties can be overcome by adding a mean field of sea height to allow for differentiation of fronts and rings. However, since one of the objectives of this study is to also investigate the volume of the rings from the displacement of the 20°C isotherm, the rings are investigated here in terms of their upper layer thickness signatures and not in terms of their sea surface height signatures. The understanding of the relationship between the sea surface height signal and the upper ocean thermal and dynamic structures is a key to assessing the limitations of altimeter-derived sea height anomaly data. The reader is referred to a previous study (Mayer *et al*, 2002) and to the chapter by Mayer *et al*, which address this topic thoughtfully by combining T/P data and XBT observations. Results presented in that chapter indicate that the sea height anomalies can be used as a proxy to investigate the upper ocean dynamics in the NBCR region.

The sea height anomaly data together with historical hydrographic data is used here to estimate the upper layer thickness. In a baroclinic ocean, each change in thermocline depth will be compensated by a change in sea level. Using a two layer model approximation, the upper layer thickness,  $h_1$ , is (Goni *et al*, 1996):

$$h_1(x, y, t) = \bar{h}_1(x, y) + 1/\bar{\varepsilon}(x, y)[\eta'(x, y, t) - \bar{B}'(x, y)], \quad (3)$$

where  $\bar{h}_1$  is the mean upper layer thickness, and  $\bar{B}'$  is the barotropic contribution to the sea height anomaly. This last parameter can be estimated, for example, when simultaneous observations of sea height anomaly and thermocline depth are available (Goni *et al*, 1996). In this study,  $\bar{B}'$  is computed using the available XBT data in the region, and is estimated to have an amplitude of 2 cm.

We present here a comparison between altimeter-derived and XBT-derived upper layer thickness estimates to show the reliability of this methodology to estimate the upper layer thickness and, hence, to identify, track and estimate properties of warm rings. Approximately 2,000 values of upper layer thickness derived from XBT data during 1993 through 2000 in the region of study were used. The XBT-derived values were extracted within 10 days of the altimeter-derived dates. The rms difference between the XBT observations and the altimeter-derived estimates of the upper layer thickness for all the observations is approximately 15 m. This difference becomes smaller when only data for warm rings (excluding subsurface rings) is used. Upper layer thickness deviations due to the passage of a warm ring range from 0 to 50 meters, with the lower value of 0 m generally observed in the subsurface rings, in which case a colder isotherm (15°C or 10°C) better reflects the isotherm deviation caused by this type of ring (Garraffo *et al*, this volume). These values indicate that the sea height anomaly can provide a fairly reasonable estimate of the upper layer thickness. The XBT observations presented here also correspond to the data used to estimate the barotropic contribution to the sea height anomaly,  $\bar{B}'$ .

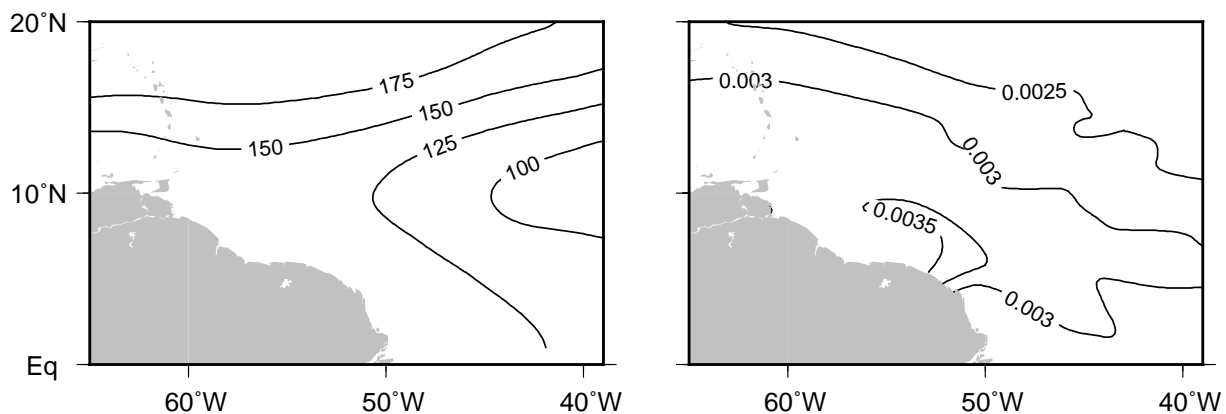


Figure 7. (left) Climatologically-derived upper layer thickness, (right) climatologically-derived reduced gravity.

## 5. RESULTS AND DISCUSSION

### 5.1. Upper layer thickness fields

Daily maps of sea height anomalies are constructed from the altimeter data covering a ten-day period centered at each day. These maps are interpolated into a regular 1/4-degree grid using a Gaussian interpolator with a radius of interpolation of 1/4 degree. The sea height anomaly maps are converted into upper layer thickness maps using (3). These maps are then used to identify and study the retroflection and the warm rings in the region. This methodology has been extensively validated in different regions such as the Brazil-Malvinas confluence (Goni *et al*, 1996), the Agulhas retroflection (Goni *et al*, 1997), the Gulf of Mexico (Shay *et al*, 2000), and the Kuroshio Extension (Sainz-Trapaga, *et al*, 2001). These maps show the North Brazil Current retroflection and warm rings in the region, distinguishable by their larger values of upper layer thickness than their surrounding waters. The close correspondence observed between the altimeter-derived and hydrographically-derived upper layer thickness maps is evidenced by the mean difference between them, approximately 5 m, with an rms difference of 15 m. Since the XBT provided observations at different times and locations than the closest altimeter observations, the errors estimated here represent an upper limit of what the actual errors actually are.

Two examples that include six maps of sea height anomalies and upper-layer thickness each are presented here to how rings are detected and tracked. Blended data from the three altimeters were used (Figure 9), where warm rings

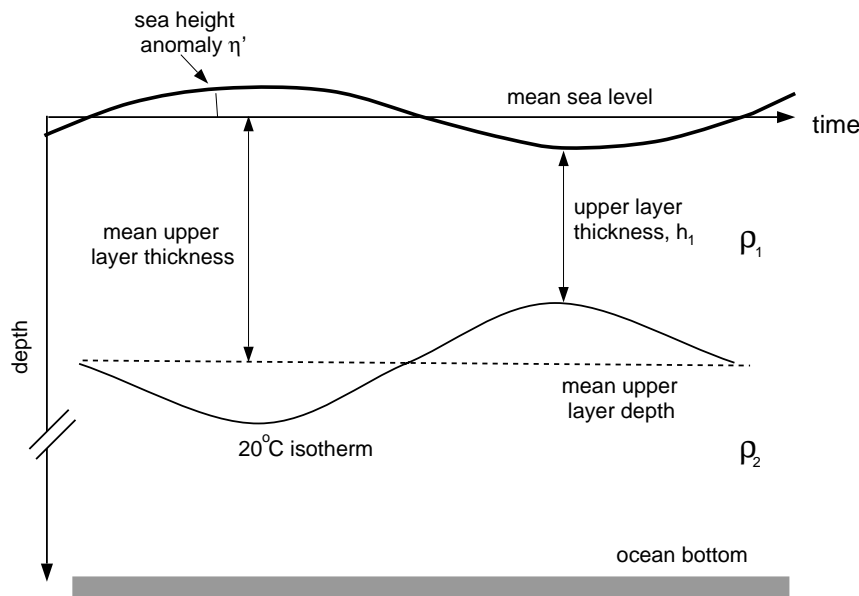


Figure 8. Schematics of the two-layer reduced gravity approximation, with an upper layer of mean density  $\rho_1$ , thickness  $h_1$  that extends to the depth of the 20°C isotherm and a lower layer with mean density  $\rho_2$ . The ocean surface has a sea height anomaly  $\eta^1$ .

are identified as closed contours in the upper layer thickness maps. Since the two-layer scheme provides better results where there is at least weak stratification, only the contours that correspond to depths characteristic of NBC rings are presented, some of which may lie within the region north of 15°N that is not of interest in this study.

In the first example (Figure 9a), a ring is shed from the retroflection during the beginning of January 1999, with the retroflection represented by a region of larger upper layer thickness values. The trajectory of this ring closely follows the bathymetry contour and is no longer detected by altimetry by late February, where another ring has already been shed by the retroflection. This ring is also identified from current meter observations (ring #2 in Johns *et al*, this volume). The second ring reaches the southern portion of the Windward Island by mid April. In the second example (Figure 9b), a region with large positive sea height anomaly values is located at 50°W, 7°N, which corresponds to the shedding of a ring approximately during mid January 2000; when the retroflection reaches its northernmost location. The translation of this ring can be followed for four months until May 2000 when it finally reaches the Caribbean Sea. This ring has sea height anomalies of approximately 12 cm and upper layer thickness variations of 50 m, within the range of typical values for most rings identified in the region. This ring is also identified from current meter observations (ring #10 in Johns *et al*, this volume). A second feature to the south that appears in the mid February map belongs to the retroflection, which later sheds a ring, and becomes more noticeable during mid March. The ring from the second example and its trajectory has been already investigated using its ocean color signature (Fratantoni and Glickson, 2002, their ring K) and is further investigated in a later section and in other chapters (Johns *et al* and Garzoli *et al*, this volume). The centers of the rings, or trajectories, are placed at approximately the geometrical center of the closed contours with the best-resolved rings, a fairly good approximation given the uncertainties involved from using the altimeters' along track data. Maps derived from the methodology presented in the previous section and similar to those shown in Figure 9 are used to identify and track all the warm rings in the region between October 1992 and December 2001. Rings translate at different speed and change speed and shape while they translate, as evidenced in the example shown here. Although these changes can be observed to some degree with altimetry, the component of these changes due to actual variations versus uncertainties in the data and the interpolation of the irregularly distributed data remains to be investigated.

The recently discovered subsurface rings have a very weak sea height signal, a characteristic also reproduced by numerical models (Garraffo *et al*, this volume), which makes them very difficult to even detect in altimetry. Several of these subsurface rings were probably not detected in our survey. A previous study (Goni and Johns, 2001) highlighted several rings that were detected during periods when the retroflection could not be identified from altimetry, and were named 'NBC eddies' to differentiate them from those shed when the NBC retroflection was positively identified. These eddies are mostly formed during

the spring months (Goni and Johns, 2000), which also corresponds to periods of time when the mean sea surface height has negative values south of the latitude of ring shedding (Figure 5, center panel). Observations (Garzoli *et al.*, this volume) indicate that the retroflection in fact exists during the spring month and this eddies may therefore be a weak surface height expression of the retroflection translated into the methodology used here. These NBC eddies are hereafter included together with the NBC rings. In addition, 12 eddies were also observed traveling in the region, not coming from the NBC retroflection but generated in the shear zone between the NEC and the NECC. These types of eddies were previously reported (DS93) and, although shown in this work, will not be included in the ring analysis or statistics. The methodology used in this work identifies most of the warm rings, except for some catalogued as subsurface. The survey presented here mostly agrees with another study that identified the warm rings using color SeaWiFs data (Fratantoni and Glickson, 2002). The color signature of the warm rings is set by the high gradient of ocean color at their edge, which is given by the large concentration of nutrients rich Amazon River waters surrounding them.

## **5.2. Ring shedding**

A total of 52 rings were observed to shed between October 1992 and December 2001 (Figure 10, top). Previously, five additional rings had also been observed during a 2.5-year period, in which observations were available, between 1987 and 1989 (DS93). Due to differences in techniques and data availability the results of the previous two studies (DS93 and GJ01) may not be directly compared, but they are both included here for completeness. North Brazil Current rings were shed every year, from a minimum of three rings (years 1988 and 1995) to a maximum of seven rings (year 1996, 1997, 1998, and 2000). The mean number of rings shed is approximately 5 to 6 per year, with a marked year-to-year variability. Although NBC rings are shed at any time of the year, they seem to have a weak tendency to form during the first half of the year (Figure 10, bottom).

## **5.3. Ring trajectories**

Most of the 52 rings are first detected between 6 and 8°N, with trajectories in the NW direction. Figure 11 shows a map with the trajectories of all the rings identified between November 1992 and December 2001. In general, these rings have their trajectories, denoted by the location of their centers, over regions deeper than 3000 m. Once the rings reach 58°W they usually turn suddenly to the North passing east of Barbados. Although this is the most common trajectory of the rings, only one out of the seven rings formed in 1996 actually followed this trajectory.

Topography has already been shown to be a very important factor in the translation of warm rings, as in the case of the Agulhas rings, which have been

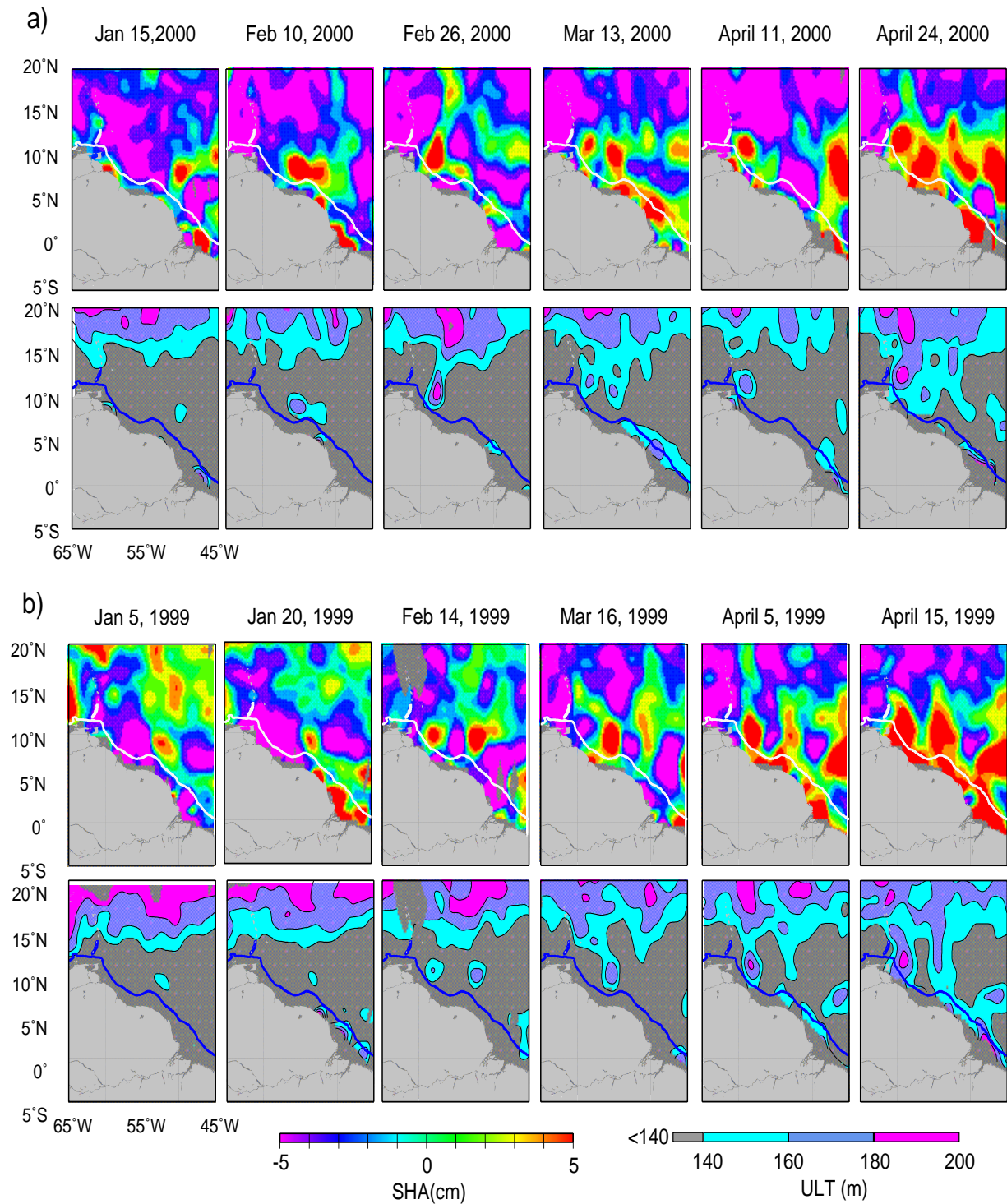


Figure 9. **(a)** Sea height anomalies (upper panels) and upper layer thickness (lower panels) fields derived from blended altimeter data from (left) January 1999 until (right) April 1999 **(b)** Sea height anomalies (upper panels) and upper layer thickness (lower panels) fields derived from blended altimeter data from (left) January 2000 until (right) April 2000. The 500 m isobath is superimposed to the maps.

shown to travel trajectories highly dominated by topography, particularly by the Walvis Ridge (Byrne *et al*, 1995; Goni *et al*, 1997; Schouten *et al*, 2000). The topography is included in the figure of the ring trajectories to help visualize the effect of the bathymetry on the ring trajectories. DS93 found that the trajectory of several rings follow the shape of the continental shelf, the 500 m contour of the bottom topography. This result was later confirmed by GJ01 where it was shown that the center of the rings approximately follow the 3000 m isobath, suggesting that most NBC rings may have vertical density signatures that go deeper than the 20°C isotherm used in this work. Almost none of the 52 rings identified in this study was observed to travel in waters shallower than 2000 m before interacting with the topography of the Lesser Antilles. The time the rings remained in the region of study ranges from two to five months, with most of the rings (27) remaining in the region for an average 3.5 months. Rings that cross into the Caribbean Sea were observed to have larger mean translation speed than the rest of the rings.

Of special interest are the rings that interact strongly with the islands of the Eastern Caribbean, particularly Barbados, since the properties carried by their waters greatly affect the environment surrounding the island, (Kelly *et al*, 2000; and Cowen *et al*, this volume). The discharge of Amazon River waters into the Atlantic Ocean peaks during the months of May and June, and the rings take approximately two to three months to travel from the retroflection to Barbados.

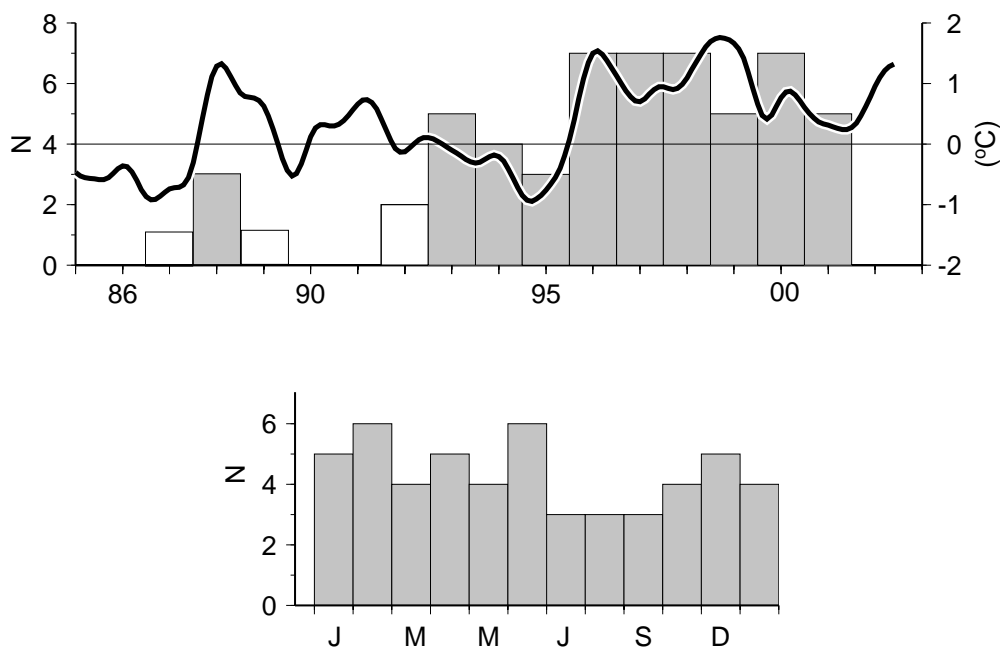


Figure 10. (top) Number of rings shed per year derived using GEOSAT (DS93) and blended altimeter (this study) data (GJ). The white bars indicate partial results because of altimeter data were not available during all the year. The (smoothed) northern tropical Atlantic index is superimposed. (bottom) Number of rings shed every month as observed from altimeter data since November 1992.

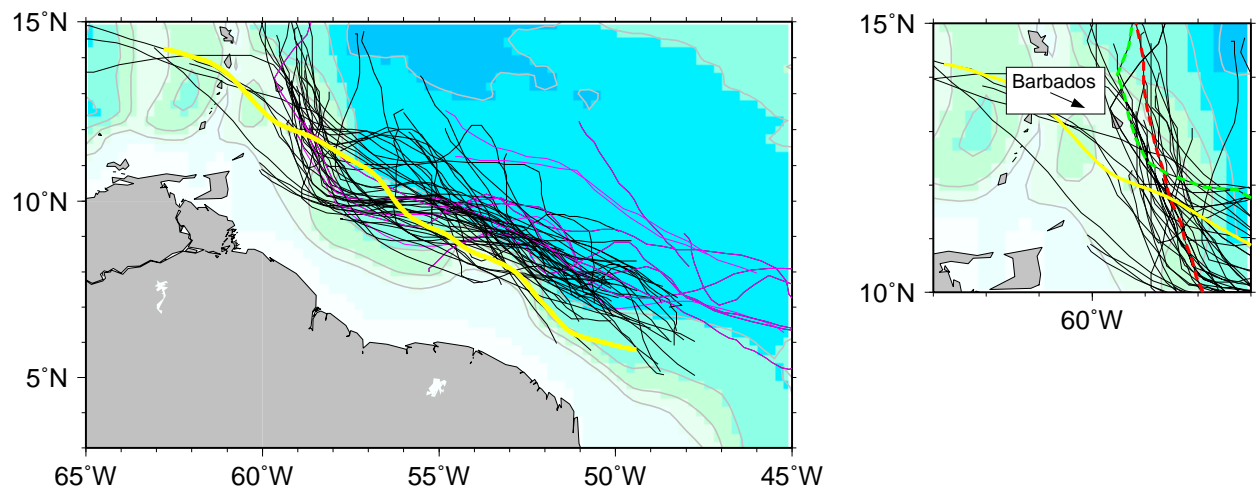


Figure 11. (left) Altimeter-derived ring trajectories from 1992 through 2001. The yellow trajectory corresponds to the ring of Figure 9b, the trajectories in purple to the eddies identified in this study. (right) Detail of altimeter-derived ring trajectories in the vicinity of the island of Barbados. The trajectory in yellow is the same as of the map on the left, while the ones in green and red correspond to the two rings studied in the chapter by Cowen *et al.* The bathymetry is included, with contours every 1000 m.

Therefore, it would be expected that rings traveling in the region of Barbados between May and September would have a larger impact in the environment of the region. This study indicates that the center of most NBC rings travel within 100 km to Barbados (Figure 11, right map). Seven rings clearly cross through the Windward Islands into the Caribbean Sea through waters shallower than 2000 m, a depth where rings are usually not found east of the Windward Islands. Once these rings cross into the Caribbean Sea, they disintegrate or their surface signal become too small to be identified with the methodology used in this study. More information on rings that enter into the Caribbean Sea and investigated using a numerical model can be found in the chapter by Garraffo *et al.* Our results indicate that none of the eddies originated in the shear zone between the NECC and NEC enter in the Caribbean Sea.

#### 5.4. Ring parameters.

The translation speed of a ring is a combination of the propagation speed of the ring and the background flow speed. The mean translation speed of the rings as obtained from the upper layer thickness maps range from 9 to 30 cm/s (7.5 to 24 km/day), with a standard deviation of 6 cm/s, which falls within the ranges of previous altimeter estimates of 15 cm/s (DS93), and 14 cm/s (Goni and Johns, 2001).

The investigation of the number of rings and their seasonal variability represent only one aspect in the study of the transfer of south Atlantic waters into the northern hemisphere. A detailed analysis of the vertical structure of these rings is also desirable. The length scale of the rings,  $L$ , are estimated here using the alongtrack sea height anomalies following the methodology used by

Goni *et al* (1997) to investigate Agulhas rings. As an approximation, these profiles are assumed to have a Gaussian shape:

$$h_1(r) - h_\infty = h_0 e^{-r^2/2L^2} \quad (4)$$

where  $r$  is the alongtrack distance measured from the center of the ring,  $h_1$  is the alongtrack upper layer thickness,  $h_0$  is the maximum alongtrack upper layer thickness depth measured from the depth of the 20°C of the surrounding waters,  $h_\infty$ , and  $L$  is the length scale. Because only two ascending T/P groundtracks, t301 and t304, are used to compute  $L$ , these estimates correspond to a region just west of the retroflexion and close in time and space to when the rings were shed. This methodology assumes that the rings are crossed by either altimeter groundtracks through their centers. Therefore, the values obtained here may be underestimated. The parameter  $h_\infty$  is computed from the upper layer thickness profiles north of the rings, where altimeter estimates are less likely to have errors related to shallow water effects, such as tides. An example is presented here with a fit along the groundtrack t304 of the altimeter-derived upper layer thickness during February 10, 2000 (Figure 9b), giving values of  $L \approx 110$  km,  $h_0 \approx 30$  m, and  $h_\infty \approx 120$  m (Figure 12). These values can change as the ring translates. The mean value for the 52 rings identified by altimetry is 100 km with a standard deviation of 27 km. DS93 estimated the radius of the NBC rings using SHA data and defining this parameter as the distance from the ring center to the location of half the maximum SHA. The mean value of  $L$  parameter for the 5 surveyed rings by DS93 using this methodology is 127 km. The length scale,  $L$ , investigated here is similar to the one presented in the chapter by Garraffo *et al*, that corresponds to the distance of the center of the ring to the radius of maximum velocity. Given that these rings may also have a barotropic or a deeper baroclinic component, which cause the dynamic properties to be translated into deeper waters, a water mass analysis is probably one of the best techniques to better estimate the amount of South Atlantic waters carried by each ring (Johns *et al*, this volume).

The volume anomaly of a ring is defined here as the excess of water (referenced to the surrounding waters) warmer than 20°C that the NBC rings carry. For rings with a Gaussian section shape (4), the volume anomaly is that of a cylinder of radius  $L$  and depth  $h_0$  (Goni *et al*, 1997). The volume anomaly for the ring presented in Figures 9 and 12 is approximately  $4.5 \times 10^{12} \text{ m}^3$ . The mean volume anomaly of all the rings surveyed in this study is  $3 \times 10^{12} \text{ m}^3$ . It is critical to understand that the volume estimates does not reflect the actual volume of South Atlantic waters carried by the rings, but rather the excess of water mass warmer than 20°C. An investigation on the ratio between the total water mass and south Atlantic water mass in rings based on both observations and model results is presented in a different chapter (Johns *et al* and Garraffo *et al*, this volume).

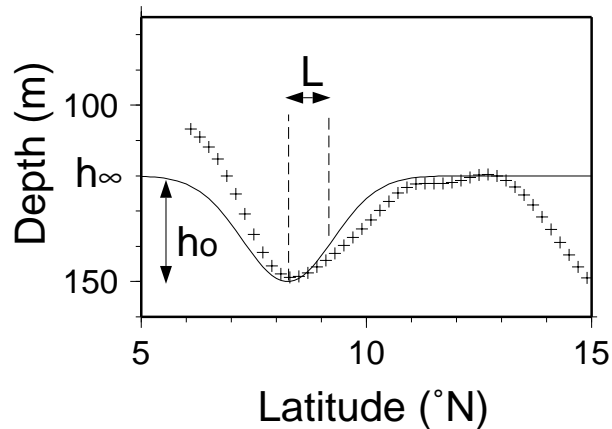


Figure 12. Upper layer thickness section corresponding to the ring of Figure 10 along t304 during mid March 2000. The crosses represent the altimeter-derived upper layer thickness values, while the solid line is the Gaussian fit (4) to these estimates.

### 5.5 Interannual variability

The cause of the interannual variability in ring formation is unknown but may be linked to other larger-scale transport processes in the basin. Larger-scale aspects of the variability in the tropical western Atlantic Ocean has been investigated from the upper ocean temperature and altimeter observations. Sea surface temperature variability has been shown to have a seasonal signal caused by surface heat fluxes and an interannual signal believed to be caused by an ocean-atmospheric positive feedback through the long wave radiation (Wang and Enfield, 2001).

These warm and cold events in the Atlantic Ocean have been correlated to the intensification and weakening of the surface currents in the equatorial region, including the SEC, through the changes in the wind fields in the tropical Atlantic (Goes and Wainer, 2002). The transport of the SEC has been shown to be larger during warming periods and lower during cooling periods. The mass transport of the SEC will clearly affect the variability of the NBC, whose transport has already been linked to the shedding of NBC rings (Garzoli *et al*, this volume). Therefore, it is speculated here that at least a weak relationship exist between the warm and cold events and the generation of rings. We use here the northern tropical Atlantic index (Figure 10, Servain, personal communication) to investigate possible links between warm and cool periods with the shedding of rings. This thermal index is obtained by the monthly standardized anomalies referenced to temperature values from 1964 until 2001 in a region of the north Atlantic bounded by 60°W-15°E, 5°N-30°N. The time series of this index shows very distinctive time periods, with amplitudes of up to 4°C. Of particular interest for this study are the warming events during 1985 through mid 1987 and during 1995 through 1999, and the cooling periods from 1988 through 1995.

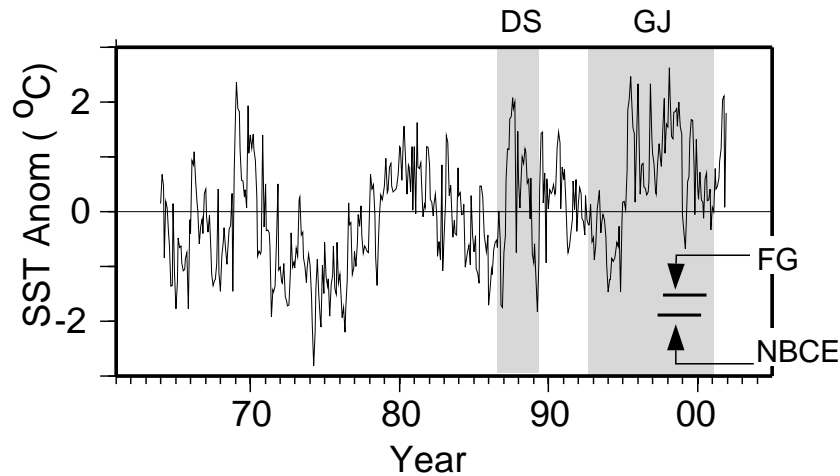


Figure 13. Time series of the northern tropical Atlantic index, given by the anomalies of the sea surface temperature anomalies. The time periods corresponding to the works of Didden and Schott (1993, DS93), Goni and Johns (2002, GJ02), North Brazil Current Experiment (NBCE), Fratantoni and Glickson (FG, 2002), and this study (GJ03) are indicated in the figure.

These cooling and warming periods can also be observed in the space-time diagrams of sea height anomalies and residues (Figure 5) as reflected by the alternation of the extreme low and high values of these parameters. Although the altimeter signal represents an integration of the dynamic and thermal effects in the water column while the thermal index is only representative of the surface conditions, their variability are qualitatively similar.

The earlier study of ring shedding (DS93) that used a shorter time series identified a smaller number of rings, only 3 rings during 1988, which corresponds to the end of a cooling period (Figure 13). Although the time series presented in this work is rather short, extending only a nine-year period (plus two of DS93), a longer time series is needed to make more definite statement to confirm this result. The shedding of rings in other regions has also been shown to be intermittent and dependent of surface current variability. For example, Agulhas rings have been closely linked to the variation of the Agulhas Current (Goni *et al*, 1997) and to the Natal Pulses (DeRuijter *et al*, 2001), creating long periods of time (8 months during 1993) when no ring was shed at all.

Results presented here will be used to validate those from numerical modeling. The long time series already being obtained using remote sensing data, hydrographic observations and models will aid in providing a clearer understanding of the role of the NBC rings in the Meridional Overturning Circulation, and on regional variability of climate patterns. As longer time series, new process studies and methodologies are incorporated there will be a more clear understanding of the mechanisms by which the NBC rings are generated and their impact in regional ocean dynamics.

## 6. SUMMARY

Ten years of altimeter data were used to investigate the temporal variability of the ring shedding in the North Brazil Current retroflection region. The ring trajectories are identified from upper layer thickness maps. Results presented here indicate a shedding rate of 3 to 7 rings per year with no marked seasonal variability but with very strong year-to-year variability. Additionally, eddies not shed by the retroflection are identified in this region as well. Most of the rings pass very near of Barbados of which seven rings during the study period are seen to enter into the Caribbean Sea. A link is found in this study between long-term surface temperature changes in the tropical Atlantic and the number of rings shed at the NBC retroflection, where periods of time with warmer surface temperatures are associated to a higher number of rings shed.

## Acknowledgements

This work was partly funded by NOAA/AOML and by NSF. Robert Cheney (NOAA/NESDIS) provided the alongtrack T/P altimetry data. The blended altimeter data was obtained from the Navoceanio web site. The northern tropical Atlantic index was provided by Jacques Servain. The authors acknowledge the comments provided by Silvia L. Garzoli during the writing of this manuscript. The authors also want to thank the two reviewers of this manuscript for their very helpful comments.

## REFERENCES

- Arnault, S. and R.E. Cheney, Tropical Atlantic sea level variability from Geosat (1985--1989), *J. Geophys. Res.*, **99**, 18207-18223, 1994.
- Byrne, D.A., A.L Gordon and W.F. Haxby. Agulhas eddies, A Synoptic view using Geosat ERM Data, *J. Phys. Oceanogr.*, **25**, 902-917, 1995.
- Conkright, M. E., S. Levitus, T. O'Brien, T. P. Boyer, C. Stephens, D. Johnson, L. Stathoplos, O. Baranova, J. Antonov, R. Gelfeld, J. Burney, J. Rochester and C. Forgy. World Ocean Database 1998, Nat. Oceanogr. Data Center Internal Rep., 14, pp. 113, 1998.
- DeRuijter W. P.O. M., H. Ridderinkhof, J. R. E. Lutjeharms, M.W. Schouten, and C. Veth. Observations of flow in the Mozambique Channel, *Geophys. Res. Lett.*, **29**, 2002.
- Didden, N. and F. Schott. Eddies in the North Brazil Current retroflection region observed by GEOSAT altimetry, *J. Geophys. Res.*, **98**, 20121-20131, 1993.
- Fratantoni, D. M, W. E. Johns and T. L. Townsend. Rings of the North Brazil Current: Their structure and behavior inferred from observations and numerical simulations, *J. Geophys. Res.*, **100**, 10633-10654, 1995.

- Fratantoni, D. M. and D. A. Glickson. North Brazil Current Ring Generation and Evolution Observed with SeaWiFs, *J. Phys. Oceanogr.*, **32**, 1058-1074, 2002.
- Goes M. and I. C. Wainer. Equatorial currents transport changes for extreme warm and cold events in the Atlantic Ocean, *Geophys. Res. Lett.*, (in press), 2002
- Goni, G. J. and W. E. Johns. A Census of North Brazil Current Rings observed from TOPEX/Poseidon Altimetry: 1992-1998, *J. Geophys. Res.*, **28**, 1-4, 2001.
- Goni, G. J., S. L. Garzoli, A. J. Roubicek, D. B. Olson and O. B. Brown. Agulhas Ring Dynamics from TOPEX/Poseidon Satellite Altimeter Data, *J. Mar. Res.*, **55**, 861-883, 1997.
- Goni, G.J., S. Kamholz, S.L. Garzoli, and D.B. Olson. Dynamics of the Brazil/Malvinas Confluence based on inverted echo sounders and altimetry. *J. Geophys. Res.*, **101**, 16,273-16,289 1996.
- Johns, W. E., T. N. Lee, F. A. Schott, R. J. Zantopp and R. H. Evans. The North Brazil Current retroflection: Seasonal structure and eddy variability, *J. Geophys. Res.*, **95**, 22103-22120, 1990.
- Johns, W. E., T. N. Lee, R. C. Beardsley, J. Candela, R. Limeburner and B. Castro. Annual Cycle and Variability of the North Brazil Current, *J. Phys. Oceanogr.*, **28**, 103-128, 1998.
- Kelly, P. S., K. M. M. Lwiza, R. K. Cowen and G. J. Goni. Low-salinity pools at Barbados, West Indies: Their origin, frequency and variability, *J. Geophys. Res.*, **105**, 19699-19708, 2000.
- Mayer, D. A., R. L. Molinari, M. O. Baringer, and G. J. Goni, Transition regions and their role in the relationship between sea surface height and subsurface temperature structure in the Atlantic Ocean, *Geophys. Res. Lett.*, **28**, 3943-3946, 2001.
- Mayer, D. A., and R. H. Weisberg, A description of COADS surface meteorological fields and the implied Sverdrup transports for the Atlantic Ocean from 30° S to 60° N, *J. Phys. Oceanogr.*, **23**, 2201-2221, 1993.
- Molinari, R. L., and E. Johns. Upper layer temperature structure of the western tropical Atlantic, *J. Geophys. Res.*, **99**, 18225-18233, 1994.
- Reverdin, G., P. Delécluse, C. Lévy, P. Andrich, A. Morlière, and J.M. Verstraete, The near surface tropical Atlantic in 1982-1984. Results from a numerical simulation and a data analysis, *Prog. Oceanogr.*, **27**, 273-340, 1991.
- Sainz-Trapaga, S.M., G. J. Goni, and T. Sugimoto. Identification of the Kuroshio Extension, its bifurcation and northern branch from altimetry and hydrographic data during October 1992-August 1999: Spatial and temporal variability. *Geophys. Res. Lett.*, **28**, 1759-1762 2001
- Schott, F.A., J. Fischer and L. Stramma, 1998. Transports and pathways of the upper-layer circulation in the western tropical Atlantic, *J. Phys. Oceanogr.*, **28**, 1904-1928
- Schouten, M. W., W.P.M. de Ruijter and P.J. van Leeuwen, *J. Geophys. Res.*, **105**, 21,913-21,925, 2000.

- Shay, L.K., G. J. Goni and P. G. Black: Effects of Warm Oceanic Features on Hurricane Opal , *Month. Weath. Rev.*, **128**, 131-148, 2000.
- Wang, C. and D. B. Enfield. The tropical Western Hemispheric Warm Pool, *Geophys. Res. Let.*, **28**, 8, 1635, 1638, 2001.
- Wilson, D.W., W.E. Johns, and S.L. Garzoli. Velocity structure of North Brazil Current rings. *Geophys. Res. Let.*, **29**, 101029/2001GL013869, 2002